AUSTRALIAN NUCLEAR SCIENCE
AND TECHNOLOGY ORGANISATION

LUCAS HEIGHTS RESEARCH LABORATORIES

MOLTEN FUEL — COOLANT INTERACTIONS RESULTING FROM POWER TRANSIENTS IN ALUMINIUM PLATE/WATER MODERATED REACTORS

by

G.J. STORR

ABSTRACT

The behaviour of two reactors which underwent fast nuclear power transients prior to core destruction by a molten fuel-coolant interaction (MFCI) have been analysed and the results compared with measured data. The calculated spatial melt distribution and the mechanical work done during the events leads to high (≈ 250 kJ/kg) conversion efficiencies for this type of interaction when compared with molten drop experiments. A simple model for the steam explosion, using static thermodynamic properties of high temperature and pressure steam is used to calculate the dynamics of the reactors following the MFCI.

ISSN 1030-7745
ISBN 0 642 59896 7

The following descriptors have been assigned from the INIS Thesaurus to describe the subject content of this report for information retrieval purposes. For further details please refer to IAEA-INIS-12 (INIS: Manual for Indexing) and IAEA-INIS-13 (INIS: Thesaurus) published in Vienna by the International Atomic Energy Agency.

A CODES; ALUMINIUM; EXPLOSIONS; FUEL RODS; FUEL-COOLANT INTERACTIONS; HIFAR REACTOR; MELTING; MOLTEN METAL-WATER REACTIONS; NUCLEAR FUELS; NUCLEATION; REACTIVITY COEFFICIENTS; REACTOR CORES; REACTOR SAFETY; SL-1 REACTOR; SPERT-1 REACTOR; STEAM; TANKS; THERMAL EFFICIENCY; TRANSIENT OVERPOWER ACCIDENTS; TRANSIENTS; WATER HAMMER; Z CODES.

EDITORIAL NOTE

The Australian Nuclear Science and Technology Organisation (ANSTO) replaced the Australian Atomic Energy Commission (AAEC) on 27 April 1987. Reports issued after April 1987 have the prefix ANSTO with no change of the symbol (E, M, S or C) or numbering sequence.

CONTENTS

1. INTRODUCTION

The majority of safety analysis work on ANSTO's reactor HIFAR, is carried out by probabilistic risk analysis methods. However, some work has been directed at determining the consequences of specific plant failures or modes of failure, in order to determine adequate reactor safety margins (*e.g.* loss of CCA; LOCA in HIFAR) [Connolly and Clark 1986; Clancy and Connolly 1985].

The prime consideration in an accident is the off site consequences of release of radioactive material. Any attempt to mitigate these consequences will ultimately depend on the integrity of the reactor containment structures. Two possible paths to containment failure are

(i) Slow overpressurisation of containment, following a LOCA.

(ii) Missile impact, either externally or internally generated.

A main feature of the first mode of failure is that the consequences of a serious accident will occur on time scales which may allow human intervention, as calculations indicate modes of failure sequenced by events which take many seconds to hours to proceed.

The second failure mode would by definition proceed quickly but suitable production mechanisms need to be determined. External missile impact by disaster or through sabotage can be examined by probabilistic methods. A missile generated by an in-core event would require the conversion of nuclear energy to mechanical work. One well known physically identified mechanism which may achieve this conversion rapidly is the steam explosion or molten fuel-coolant interaction (MFCI).

MFCI may occur as a result of a LOCA but are probably only hazardous in power reactors where large hold up of melt can be envisaged with subsequent contact with water. Because of the large mass of melt and high temperatures, even low efficiency of conversion of melt energy to mechanical work may pose a threat to containment.

For research reactors the situation is generally different, in that metal inventory is small, the metal melting point is low, and there exists little structural arrangement to impede the flow of melt. Metal water contact would then be incoherent in a LOCA accident, and large energy release by an MFCI unlikely.

However, the same features and the high specific power (kW/kg) make a research reactor more susceptible to an MFCI induced by a reactivity accident. If fast enough, this may result in *in situ* melting of metal in the presence of water, the premixed condition to be discussed later.

The physical phenomena associated with MFCI are many and complex, however, it is well known that three reactors, BORAX 1, SL1 and SPERT D12 were destroyed by explosive phenomena following fast transient over power (TOP) events.

This report describes analyses of two of these transient events, SL1 and D12.

2. STEAM EXPLOSION MECHANISMS AND THEORIES

Two theories proposed to explain steam explosion resulting from a MFCI, have widespread support. They are the spontaneous nucleation theory and the detonation theory.

2.1 Spontaneous Nucleation Theory

The spontaneous nucleation theory proposed by Fauske [1972] requires as conditions for a large scale vapour explosion, that liquid-liquid contact must exist such that the contact interface temperature established between the molten (hot) alloy and coolant must exceed the spontaneous nucleation temperature of the coolant, *i.e.* $T_I > T_{SN}$. By using Volmer's [1945] rate equation for bubble nucleation it is seen that the nucleation rate will remain small until a threshold temperature is reached at which the vapour bubble nucleation rate escalates rapidly.

The condition $T_I > T_{SN}$ was redefined by Bankoff [1980] to mean local pressurisation occurs immediately upon contact of the two liquids. This takes into account that large scale explosions have been shown to proceed when the inter-face temperature is greater than the coolant critical temperature.

The theory relies on the coolant nucleating rapidly once a fine-scale fragmentation and intermixing is achieved. The rapid vapour production causes shock pressurisation of the system; a steam explosion occurs.

One well known physical configuration which may lead to a steam explosion is when the coolant is trapped by the molten metal; a so-called entrapment explosion. This type of explosion has been observed to occur without a triggering mechanism and is an indication that the Spontaneous Nucleation theory may be correct. In a reactor situation it is easy to envisage plates distorting to the extent where they trap water in the channels and as the reactivity transient proceeds the metal melts providing liquid-liquid contact.

2.2 Multiphase Detonation Theory

Board *et al.* [1975], in a one-dimensional model treats the propagation of a steam explosion in a manner similar to the behaviour of a shock wave during a chemical detonation. The theory assumes a strong shock front propagates steadily through a coarsely mixed medium of molten metal, coolant and coolant vapour. As the shock progresses vapour blankets collapse, and flow velocity differences between the denser liquid and lighter coolant cause fine scale fragmentation by hydrodynamic instabilities of the hot material followed by rapid heat transfer. The material behind the front is now considered to be in thermal equilibrium at high pressure, and this high pressure drives the shock wave forward.

For this theory to be physically realistic an initiating shock must occur, the so-called triggering event.

A common sequence of events may be incorporated by both theories to explain an MFCI. They are:

1. Fuel coolant premixing, with stable film boiling.
2. Collapse of stable film boiling.
3. Fuel coolant contact, with rapid vapour production and shock pressurisation.
4. Expansion of vapour, and macroscopic propagation of the event.

2.3 Efficiency of Interaction

Estimates of the efficiency of MFCI's have been made from measurements in a variety of experiments and some are listed in **Table 1** [El Genk *et al* 1987]. The overall conversion efficiency (ratio of mechanical work done to energy available for an interaction) of an interaction varies widely for different melt, coolant and system geometry. As such the efficiency of an interaction in say, a molten drop type experiment may not describe the interactions experienced in a plate type reactor geometry.

It has been observed that many molten drop experiments do not proceed to an MFCI and explosion. It is believed that the mode of molten fuel breakup (fuel-coolant pre-mixing) may determine whether an interaction proceeds in a random geometry melt situation. A significant difference exists in a reactivity accident that is fast enough to allow "in situ" fuel melting as a defined geometry of molten fuel and water may be established before fuel breakup occurs. Even if plate deformation occurs, the fuel and coolant will still be pre-mixed.

Many questions remain unresolved in this large and complex field of research. This report ignores the mechanisms involved in obtaining an MFCI and concentrates on calculating the correct reactor conditions, comparing the mechanical effects produced by the steam explosion to these conditions thus allowing an estimate of the efficiency of an MFCI in these circumstances.

TABLE 1
CONVERSION EFFICIENCIES FOR MFCI EXPERIMENTS WITH WATER COOLANT

Experiment	Melt	Overall Conversion Efficiency (%)
Sandia, FITS	Fe/Al_2O_3	1.1-2.1
Sandia, single drop	FeO_{1+x}	2.7
Shock tube (Kottowiski)	Stainless steel	0.2-2.6
RIA - ST-4	UO_2/Zircaloy mixture	0.3
Shock tube (Anderson and Armstrong)	Aluminium	5.0-25.0
Underwater melt release	UO_2	6.0

3. BRIEF DESCRIPTION OF SL1 AND SPERT D12 REACTORS AND THE REACTIVITY EVENTS

Descriptions of both reactors and the circumstances surrounding the destruction of their cores is recorded in detail elsewhere [SL1 Report Task Force 1962; Miller *et al.* 1964]. **Figure 1** shows scaled schematics of SL1, D12 and HIFAR vessels and cores, whilst **figure 2** shows scaled schematics of core cross-sections of the reactors. The SL1 and DI2 cores were light water moderated with Al/U plate type fuel, and both suffered TOP events after the withdrawal of a central absorber. **Table 2** gives some data on the two reactors.

TABLE 2
PARAMETERS FOR SL1 AND SPERT D12

		SL1	D12
No. of fuel elements		40	25
Fuel plates/element		9	12
^{235}U/fuel plate	(g)	38.9	14.0
^{235}U core mass (clean)	(kg)	14.0	3.8
Water gap	(cm)	0.7874	0.457
Cladding thickness	(cm)	0.0889	0.0508
Alloy thickness	(cm)	0.127	0.0508
Core metal/water volume ratio		0.386	0.334
Vessel height	(m)	4.42	4.65
Vessel diameter	(m)	1.33	3.05

The SL1 accident is believed to have been initiated by the manual withdrawal of the central control rod (see **figure 2**), an event which sent the reactor prompt supercritical. The nuclear energy release was rapid enough to melt much of the central core fuel plates, where it is hypothesised [Jackson *et al* 1988; El-Genk *et al* 1987] an MFCI occurred, which led directly to the destruction of the reactor and the deaths of three operators.

The destructive test run on SPERT1 D12 core was initiated by the expulsion of a central 'transient' absorber rod from the core. The nuclear characteristics of the shutdown were due to fuel and moderator thermal expansion and boiling. Some 15 msec after the measured power peak, and after the reactor was effectively shutdown, there was a rapid pressure rise, probably due to an MFCI that destroyed the reactor.

4. REACTOR CALCULATIONS UP TO THE TIME OF MFCI

One of the objectives of the investigation was an attempt to calculate from first principles the conditions experienced in the reactors under reactivity transient conditions. The ability to calculate events which give good comparisons with observed conditions in the reactors is of importance to give credence to HIFAR safety studies.

Previous work [Clancy *et al.* 1975, 1976] showed good agreement between calculated and measured data of the SPERT series of reactor tests. Whilst the emphasis in these reports lay on the power burst behaviour and the reactivity feedback effects, the present work extends the analysis to fuel melting and therefore a simple model for metal melting.

Calculating reactor behaviour from initiation of the reactivity transient up to the time of the MFCI relied on neutronics calculations *via* the AUS code [Robinson 1987], to obtain necessary parameters needed for transient analysis by the ZAPP code [Clancy 1983].

A brief description of the modelling of core neutronics and transient analysis is given in **Appendix A.** In the case of SL1 the AUS calculations confirmed the central control rod criticality hypothesis.

4.1 Data on Reactor Events

Table 3 gives a qualitative description of known facts about the SL1 and D12 reactor events. The data is from direct observation or inferred from measurements.

TABLE 3
QUALITATIVE RANKING OF DATA

Quality Rank	SL1	D12
Good	Total nuclear energy release Mechanical work done	Total nuclear energy release* Reactivity inserted Time of explosion
Fair	Reactivity inserted Mass of fuel melted	Mass of fuel melted Form of power pulse
Not known or poor	Time of explosion Form of power pulse Temperatures at time of explosion	Mechanical work done Temperatures at time of explosion

* A question arises for the recorded power trace, as it appears it may have been distorted due to the high void content in the core (see **section 4.2**).

4.2 Comparison of Calculated and Measured Parameters

Table 4 shows comparisons of some of the present analysis calculated results with data either measured directly or inferred from the post event evidence for the SL1 and D12 transients. Much of the SL1 observed data, is cited by the major analysis done on the SL1 accident [Kunze 1962].

TABLE 4
COMPARISONS OF CALCULATION AND OBSERVED PARAMETERS IN SL1 AND D12 TRANSIENTS

		SL1		D12	
		Observation	Calculation	Observation	Calculation
Prompt neutron lifetime	(μs)	~ 60.0[a]	44.2	57.4	60.0
Inverse period	(s^{-1})	256	256[b]	313	313[i]
Maximum power	(MW)	1.9×10^4	1.9×10^4	2250	3323[e]
Time to peak power, t_M	(ms)	~ 120	95.1	~ 80.0	57.1
Energy release at t_M	(MJ)		119.5	13.8	15.6[e]
Total energy release	(MJ)	133 ± 10	209.7[c]	30.7	29.3[e]
Volume ratio metal, water water and superheated water at MFCI			1/2.5/.07		1/2/1
ZAPP zone 1 temperature	(°C)				
Alloy			1731	654	519[f]
Clad			659	539	493
Maximum fraction core molten		~ 0.32[d]	0.22	0.35[g]	0.37
Fraction core molten at MFCI		~ 0.32	0.22		0.06
Quantity molten metal at MFCI	(kg)	~ 61	42.6 ± 4.2		4.8 ± 1.0
Energy partition: molten metal/water	(MJ)[h]		58.1/0.4		4.6/0.3

(a) The observed prompt neutron lifetime is an inferred value, probably taken as the average quoted in ANL-5744 of 40-80 μs for different core conditions.

(b) Reactor period chosen for the calculation is the same as value quoted in SL1 analysis by General Electric. Since energy release is well known, the amount of material melted is not very dependant on the period.

(c) The calculated energy release indicates the reactor was destroyed by the steam explosion before the reactor was shutdown by feedback effects and after the power peak. Spatial melting was calculated using the ZAPP temperatures at an energy release of 133 MJ.

(d) The maximum fraction of core melt was assumed at the time of MFCI. The observed estimate has a significant error associated with it, due to a large portion of the core either

not recovered or unidentifiable.

(e) The total energy release comparison appears good, however, the power shapes are quite different. The observed pulse is unusual, with the back end of the pulse exhibiting "bulging", which is not characteristic of a non-linear feedback mechanism, which certainly terminated the transient. An explanation may be as the core becomes increasingly voided, the neutron leakage increases, thereby increasing the signal to the external core power detectors.

(f) The observed temperature data are inferred by extrapolation of buried thermocouple data. Due to the fast transient and extrapolation this data cannot be given great weight. The calculated temperatures were falling rapidly ($\approx$ 15,000°Cs^{-1}) at the time of the MFCI. The time of the MFCI is known accurately at 15 msec after the power peak.

(g) As the calculated temperatures were falling at the time of the explosion, the fraction of the metal molten at this time calculates less than the maximum melted. This condition is not applied in other analyses. The comparison between the calculated maximum molten fraction and that observed in the post accident analysis is excellent.

(h) The molten metal energy is calculated for the metal that melts from ambient temperature to the calculated power weighted temperature at the time of interaction. Energy in the water is for the area next to the plates that are molten at the interaction.

(i) The reactor period for the D12 test was measured accurately. The same value is used in the calculation.

Comparisons between the calculated melt pattern and the inferred melting from post event analysis is complicated by the explosions and consequent loss of material in the reactors. In SL1 the exact time of the explosion is not known, and following the argument in (c) above the calculated melt pattern at the time of the explosion is taken to be when the energy release equals 133 MJ in the ZAPP calculation.

The quantity of molten metal in the reactors was calculated from the ZAPP region temperatures in a zone, adjusted for fuel element power, and assuming an axial cosine temperature distribution given by the axial buckling used in the AUS calculations. Two limitations of this model are the inability to model geometry changes, and radial temperatures are assumed constant across a region.

Two notable differences between SLI and D12 at the time of their explosions are the partition of energy and the void fraction. In D12 about 8 per cent (2.5 MJ) of the total nuclear energy release had gone into heating water at the time of the explosion, whilst in SL1 less than 1 per cent (.9 MJ) of the total nuclear energy release had gone into heating water. At the explosion times D12 was calculated to have 35 per cent void in the core whilst SL1 was calculated at 4 per cent core voided. The thick cladding of the SL1 fuel plates effectively delayed heat flow to the coolant.

5. THE MFCI EVENTS

5.1 The SL1 MFCI

At the time of the accident in SL1 no signal recorders were operating and therefore post accident evidence was all that was available to piece together a description of the accident events. Additional knowledge was gained by scale model tests, performed in two laboratories in an attempt to model the accident events related to the steam explosion in SL1 [Warren and Rice 1965; Kunze 1962].

According to the calculations, at peak power the negative reactivity of 1.2 ρ per cent produced by temperature increase in the coolant and production of voids by steam generation was enough to reverse the power burst. About 1 msec after peak power (at the time of MFCI) the fuel had reached vaporisation temperature in approximately 10 per cent of the core and approximately 20 per cent of the clad was molten.

The MFCI was initiated, with the rapid transfer of heat from the molten fuel to the water. The core was pressurised due to steam formation, with acoustic relief coming from shock wave propagation and steam expansion away from the interaction zone.

It was demonstrated in the scale model tests that the explosion proceeded in three stages after the interaction. The first was the expansion of the lower vessel due to steam expanding next to the core, and a downward force due to the same phenomena ruptured the connecting pipework thus freeing the vessel. Secondly, the vapour explosion accelerated upwards the water above the core as a slug where it collided with the vessel top plate and caused expansion of the top portion of the vessel due to the water hammer. Thirdly, enough energy was transferred in this process to move the whole of the reactor vessel upwards an unrestricted distance of 3.3 metres. There was clear evidence of this due to indentations left in the ceiling above the vessel rest position.

The pressure measured at the head of the reactor model [Warren and Rice 1965] of 70 MPa confirmed the value deduced from the crushed control rod guide tubes examined from the actual reactor, after the accident.

5.2 The D12 MFCI

The events of the D12 destruct test were seen to follow the same general pattern as those in the SL1 accident. Film of the test showed the Cerenkov glow associated with the nuclear power burst, followed by a downward movement of the lip of the reactor vessel. This was probably due to the reactor vessel walls bulging outward and the downward force on the vessel floor due to the expansion of the steam bubble created by the MFCI. A water jet was seen to emerge from the reactor vessel after the solid periscope structures started moving upwards following the initial move downwards by the reactor vessel.

The water jet did not however appear as a slug. Rather it was well fragmented, but whether this was due to structural collisions or the nature of the explosion is not clear. The leading edge of the

water plume has been estimated in this work to have an initial velocity of 44 m s^{-1} and rose to a height of approximately 25 metres. It was observed that much of the expelled water did not reach this height.

Pressures measured external to the reactor core were of the order of 10-20 MPa inferring much higher pressures at the interaction site.

5.3 Estimates of the Mechanical Work Done During the Events

Estimates of the mechanical work done during the two events relied on examining post event evidence and calculating the mechanical work needed to perform the observed destruction. Broadly, energy was absorbed by the vessel, the core and the overlying water column in both reactors.

5.3.1 Analysis of SL1 reactor

The analysis of Proctor [1967] deducing the mechanical energy done by the steam explosion is assumed correct. Proctor's analysis evaluated the mechanical energy required to deform the reactor vessel from measurements of the deformed vessel profile and the strain energy required to do this under transient conditions. The deformations are apportioned to the initial steam expansion and the water hammer effect. Estimates are made on the energy absorbed in destroying the core structures and thermal shield. An accurate value for the energy used in projecting the vessel and components upwards was available from the post accident evidence. The total mechanical work performed in the SL1 system is taken as 6.1 MJ, apportioned in the following manner:

Absorbed by lower vessel, thermal shield and core	2.5 MJ
Absorbed from water hammer in upper vessel and head damage	3.1 MJ
Vessel jump	0.5 MJ

5.3.2 Analysis of D12 reactor

An estimate of the deformation of the reactor vessel has been made in this work from photographic evidence, given the maximum radial deformation at the core level was 3 inches [Silver, 1965]. The vessel was clearly deformed over 9 feet, with bulges showing between the externally located stiffening rings at 3, 6 and 9 feet from the vessel base. The maximum radial deformation in the rings above and below the core ring were estimated in this work to be about half the deformation of the core ring. By using a linear distribution between the maximum deformations and the tank ring stiffners (where no deformation is assumed) a total volume expansion is calculated as 0.67 m^3. Using the yield pressure of the vessel [Miller *et al* 1964] and assuming transient loading, the mechanical energy required to deform the vessel by 0.67 m^3 is calculated to be 1.29 MJ. This is however, a minimum estimate as the vessel was back-filled with earth. The D12 core volume was approximately a quarter the core volume of SL1, and if the mechanical energy absorbed is scaled directly to core volume then 0.1 MJ would have been absorbed in D12 core structures.

Any estimate of the mechanical energy imparted to the overlying water column is difficult due to the nature of the water expulsion. The finely fragmented nature of the spray and fits of the leading edge of the plume indicate that drag forces perturbed a significant portion of the water in its vertical travel. For calculation purposes it is estimated that 5000 litres was expelled during the test run. Bunch [1965] estimated that 7,500 litres was expelled, but Miller [private communication] indicated no measurements were made.

There is a likelihood that an unsupported shock wave may have been responsible for at least some of the water ejection, as shock effects were evidenced at the side and bottom of the reactor tank; all similar travel distances from the interaction zone. This is supported by the pressure estimate P just below the water surface of 8.8 MPa given by an equation describing the velocity of a free particle at the surface above an underwater explosion [Cole 1965].

$$P \cos \delta = \frac{\rho_o c_o u_z}{2} \qquad (1)$$

where δ = angle between particle and detonation point = 0

ρ_o = density of water = 10^3 kg m^{-3}

c_o = shock propagation velocity (steam explosion) = 400 m s^{-1}

u_z = velocity of free particle at surface = 44 m s^{-1}

The pressure behind a shock of this characteristic, appears in reasonable agreement with the measured higher pressures outside but closer to the D12 core. However, it is not possible to estimate the quantity of water ejected by this phenomena, as it predicates a knowledge of the efficiency of the explosive process.

An estimate of the mechanical work done to the bulk water thus becomes difficult. It is left until the analysis in **section 6** to assign an energy estimate to the water slug, by using a model for a constrained steam explosion.

6. CONDITIONS AFTER THE MFCI

6.1 Steam Explosion Debris

A characteristic of an MFCI is the fine metallic particulate residue produced by an interaction. In both SL1 and D12 significant quantities of fuel and clad particulate were found in the bottom of the reactor vessels. Samples of identifiable fuel material from both reactors were characterised by size by sieving the material through standard sieves.

Bird [1984] says that UO_2 drops of diameter less than 0.28 mm can lose heat sufficiently rapidly to produce an MFCI. The ratio of the radii of spherical droplets of aluminium and UO_2 having the same Fourier number (losing heat over the same time for MFCI) is 4.3. This implies that aluminium spheres of diameters less than ~ 1.2 mm could contribute to a MFCI. For the purposes of the study

all particulate debris below 1.4 mm (closest sieving size to 1.2 mm) was taken as interacting. In SL1 this translated to 55 per cent of melt interacting and in D12 - 65 per cent of melt interacting.

6.2 Steam Explosion Model

The model used to calculate the conditions in the reactor after the MFCI assumes instantaneous energy transfer from the molten fuel which interacts, to the coolant with the subsequent formation of steam at a predefined pressure and temperature. The thermodynamic properties of steam [Mayhew and Rogers 1970] under static temperature and pressure conditions, are assumed to be valid under the real transient conditions in the reactor. An interaction volume is defined as the volume of molten fuel interacting, the volume of water converted to high pressure and temperature steam, and the volume of superheated water adjacent to the interacting fuel prior to interaction.

The idealised interaction volume comprising molten metal and supercritical steam is allowed to expand adiabatically and deform the reactor walls. An adiabatic process is chosen, as the rapid expansion will prevent significant heat loss from the steam bubble. The mechanical energy required to do this is calculated from the vessel deformation measurements (**section 5.3**). It can be shown that the residual pressure P in the reactor, after expansion of the vessel walls, is for an adiabatic process.

$$P = \frac{W(\gamma - 1) V_0^{\gamma-1}}{V(V^{\gamma-1} - V_0^{\gamma-1})} \qquad (2)$$

where

W	is the mechanical work done in expanding vessel walls	(J)
V_o	is the interaction volume	(m^3)
V	is the interaction volume + volume of expanded walls	(m^3)
γ	is the ratio of specific heat at constant pressure to specific heat at constant volume.	

The residual pressure is then used to accelerate a quantity of water above the core to determine a water slug velocity. The expansion in this phase of the model is treated as an adiabatic one. However, if extremely rapid cooling (tens of milliseconds) were to occur due to the interactants mixing with the surrounding medium during the initial steam bubble expansion, then an isothermal expansion accelerating the water column would be the limiting case.

As the model assumes adiabatic expansion after interaction the temperature after expansion Θ, can be related to the interaction temperature Θ_o, by

$$\Theta V^{\gamma-1} = \Theta_o V_o^{\gamma-1}$$

where the other parameters have the same meaning as in equation 2. Thus if the volume expansion is very large before the water slug is allowed (in the model) to move then an isothermal expansion will again be the limiting case.

In practice the equation of state describing the conditions of the high pressure mix will be different from the assumptions used in this work however, the methods used are general.

The work energy required to accelerate the water slug is equated to the kinetic energy of the water slug movement plus the potential energy when collision or pressure relief occurs. It can be shown that the square of the velocity of the moving water column, can under adiabatic assumptions be given by,

$$v^2 = \frac{2\,P\,V^{\gamma}}{m(1-\gamma)}\left[(V + Az)^{1-\gamma} - (V)^{1-\gamma}\right] - 2\,g\,z \qquad (3)$$

where
- P = pressure in **equation 2** - the driving pressure (Pa)
- V = total volume after expansion (m^3)
- m = mass of overlying water slug in motion (kg)
- A = cross-sectional area of reactor vessel (m^2)
- z = travel distance of slug to collision or pressure relief *i.e.* water level to vessel head (m)
- g = acceleration due to gravity ($m\ s^{-2}$)
- γ = is the ratio of specific heat at constant pressure to specific heat at constant volume.

In the case of SL1, where the water slug was constrained by the vessel head an estimate of the pressure due to the water hammer can be made, given the vessel deformation in this region. The pressure calculation depends on the pressure distribution assumed through the water slug, and on the structure of the vessel walls not being perfectly rigid. For non-rigid walls a modified bulk modulus K' given by

$$K' = K/(1 + (K2r/Et)) \qquad (4)$$

where
- K = bulk modulus of water (Pa)
- r = radius of vessel (m)
- t = vessel thickness (m)
- E = elastic modulus of vessel (Pa)

is used.

The model assumes that the mechanical work done in expanding the vessel is due solely to gas expansion processes, and ignores shock effects. Evidence that this may be true, at least in SL1, is that the scale model tests showed that a vessel wall ruptured by a shock wave allowed the reactor to be depressurised quickly, before any water expulsion or vessel movement.

6.3 Results of Model Calculations

The temperature and pressure conditions chosen for the region behind the interaction front are T = 500°C and P = 70MPa. These values are chosen with justification, as the condition of rapid heat transfer [Jackson *et al* 1988] during an MFCI requires rapid metal cooling, and the pressures measured in D12 and inferred in SL1 are known to be of the order of tens of MPa external to the core. Additionally, the interface temperature has been observed as greater than the coolant critical temperature in some large scale explosions [El-Genk *et al*, 1987]; that is where melt masses were of the order of kilograms.

A check on the sensitivity of these parameters showed changing initial temperature conditions has little effect on slug velocity if the initial pressure is kept high (above 60MPa). It can be seen from **figure 3** which shows a plot of calculated water slug velocity in SL1 against initial interaction pressures for four different initial temperature conditions, that the scale model test water slug velocity of 49 ms^{-1} could be matched under adiabatic assumptions if the initial temperature condition is lowered at the expense of lowering the initial pressure. In effect the process would become a 'volume' driven expansion. There is no evidence to suggest that temperatures in the metal can fall this rapidly, and as the measured pressures external to the core in D12 were approximately equal to the pressures indicated in **figure 3** from the lower temperature plots (≈ 25MPa), it is concluded that the lower initial temperature conditions can be ruled out.

Figure 4 shows a plot of initial pressure against water slug velocity for SL1, at an initial temperature of 500°C for an adiabatic and an isothermal expansion. An equation of state to the left of the adiabatic (where a shock adiabatic would occur) would satisfy the scale model slug velocity for lower pressures than the adiabatic assumption. Clearly as successive equations of state assumptions are traversed for the measured water slug velocity, from the isothermal limit down, the required initial pressures for the steam-metal mix will decrease. The model implies that supercritical steam conditions exist at interaction which compares favourably with other large scale MFCI where the interactant coolant temperature was greater than the critical temperature [Bankoff 1980].

One of the central problems in steam explosion analysis is the attempt to describe the nature of the mixture which leads to an explosion. The model used in this report while being over simplified, is easy to manipulate theoretically and indicates directly the macroscopic nature of the steam explosions in SL1 and D12. It also points to areas of deeper investigation, and limits to the transient reactor model.

Table 5 lists the parameters calculated for SL1 and D12, under adiabatic expansion assumptions with the initial pressure at 70MPa and the temperature at 500°C.

TABLE 5

CALCULATED MFCI PARAMETERS FOR SL1 AND D12

		SL1	D12
Molten metal interacting	(kg)	23.4	3.1
Energy in metal interacting (to 500°C)	(MJ)	23.6	1.65
Energy available for MFCI	(MJ)	23.8	1.9
Volume of water converted to P = 70MPa, T = 500°C	(m^3)	0.0238	0.0019
Volume of interaction zone	(m^3)	0.0323	0.0037
Volume after vessel expansion	(m^3)	0.1173	0.6767
Driving pressure	(MPa)	13.55	0.16
Mass of water slug accelerated	(kg)	3000	5000
Velocity of water slug	($m\ s^{-1}$)	42.3	7.5
Peak impact pressure, due to water hammer	(MPa)		
linear assumption		40	
non-linear assumption		74	
Transient efficiency (mechanical work/nuclear energy)		0.046	0.055
Intrinsic conversion efficiency (mechanical work/energy available for MFCI)		0.258	0.895
Intrinsic conversion interaction efficiency (mechanical work/kg fuel interacted)(kJ/kg)		262	548

7. DISCUSSION

It was considered that because the D12 transient was a fully instrumentated test, analysis of this data would lead to a good estimate of the efficiency of the MFCI, and thus could be compared to a less accurate estimate of the SL1 efficiency in order to decide whether it was reasonable to conclude both transients involved the same basic physical phenomena. In the event, the D12 calculations produced unrealistic efficiencies; some of the difficulties are discussed below. The intrinsic conversion efficiency can be compared with the valves given in **table 1** for MFCI experiments.

7.1 The SL1 Accident

Comparison of the conversion efficiencies given in **table 5** with conversion efficiencies for various explosion experiments [El Genk *et al* 1987] indicate that the MFCI in SL1 was, in terms of a vapour explosion, very efficient. The SL1 results coincide with efficiencies for aluminium water shock tube experiments, and are consistent with efficiencies predicted by a Board Hall thermal detonation model [Fry and Robinson 1980].

The steam explosion model employed predicts with good accuracy the kinetic energy of the water slug of 3.6 MJ, if the initial pressure and temperature conditions are taken as 27 MPa and 500°C respectively. Under these conditions estimates of the pressure due to the water hammer at the vessel head assuming a linear, pressure distribution gives 52 MPa. A pressure distribution of the same general form as the vessel deformation distribution gives a peak pressure of 102 MPa over 30 cm with a pressure falling to 16.5 MPa over 61 cm. The non-uniform pressure distribution provides a good comparison with the estimated pressures experienced in the reactor given the deformation of the control rod guide tubes.

A reason for the success of the analysis for SL1 is in the assumption that the overlying water slug does not move before the vessel walls are deformed by the steam expansion. It is clear from the dimension of SL1 that acoustic relief happened first in the radial direction. This phenomena was demonstrated in the scale model tests by Warren and Rice [1965]. The scale model tests also confirm the values estimated here of water slug velocity and impact pressure of the water slug. Additionally the ZAPP calculations indicate the MFCI occurred just after peak power, probably before large scale plate deformation, which would have altered the heat transfer characteristic of the fuel.

7.2 The D12 Test

The results of the D12 calculation are questionable. The efficiencies shown in **table 5** are too high. The source of this high value is not an overestimate of the mechanical work done during the test. The calculated estimate is, as shown in **section 5.3.2**, low. Consequently the melt calculation, is in some way in error. There is no doubt that the explosion occurred 15 msec after the measured peak power, and the post test observations show that 35 per cent of the core was molten at some time during the test. There is an assumption in many papers that the maximum melting was at the time of the explosion. The ZAPP calculations do not agree. The calculations indicate that 5 msec after peak power 37 per cent of the core was molten, but by the time of the explosion temperatures were falling rapidly and only 6 per cent (5 kg) of the core was still molten.

A noticeable difference between calculation and experiment is the shape of the power burst. Comparatively the experimental power pulse is broader after peak power and the calculated power peak is higher. One explanation may be the external power detector signal is increasing because of increasing leakage as core voiding becomes large. Another solution may be that heat transfer is not being modelled correctly in ZAPP under high void fraction conditions. It is apparent that if melting is increased at explosion time the efficiencies in D12 can be forced to similar values as those calculated in SL1. By assuming an efficiency of interaction of 262 kJ/kg for D12 and taking the calculated (and observed) maximum melt, then 5000 litres of water could be expelled from the vessel at 22 m s^{-1} which approaches the average water plume ejection velocity. This implies that the mechanical work done in the D12 explosion was 3.3 MJ, which reduces the intrinsic conversion efficiency to 0.38.

The ZAPP transient model would appear to be failing for destruct transients at relatively long times after peak power. This could be quite consistent with the observations, as melting and plate deformation destroys the geometry of the core. The post accident evidence of the fuel plates clearly show gross deformations which if occurring before the MFCI, have altered the geometry of the reactor and hence the heat transport properties significantly, *e.g.* plates touching and fusing together. A process such as this would be likely to increase the energy held in the fuel, thus maintaining the melt over longer periods. Additionally, it has been postulated that film boiling proceeds an MFCI [Hall 1988], which may lead to heat transfer to the water being too high in ZAPP prior to detonation. These could be areas for future investigation.

The more open geometry of the D12 tank resulted in ambiguous data related to the mechanical work done after the MFCI. This combined with the lateness of the explosion meant a less exact analysis. However, if it is assumed that the maximum melt was held to the time of the explosion, the D12 effeciencies coincide with the SL1 results and the observed D12 plume velocity is approached.

7.3 Application to HIFAR Studies

The inferred efficiencies for MFCI events in SL1 and D12 are high enough to mean that fuel melting occasioned by a TOP event in HIFAR is not permitted. The complex geometry of the HIFAR reactor aluminium tank (RAT) with its many penetrations running close to the core, is much more vunerable than SL1 or D12.

The RAT is made of 99.8 per cent aluminium to BS1470:SIA in the half hard condition. The HIFAR Safety Document [1972] states the tank is required to withstand without rupture a design emergency lasting twenty four hours with an initial pressure of 0.22 MPa. This leads to a yield stress of 17.3 MPa. Under the transient conditions considered in this analysis the transient yield stress (0.2 per cent deformation) is 34.6 MPa and the ultimate stress is 240 MPa. Rupture would be likely to occur for pressure transients in this order of magnitude.

Figure 5 shows a diagram of the HIFAR RAT, core outline and other structures associated with the RAT. Detailed deductions about an accident of the type examined in this work in HIFAR would require an appreciable analysis of the dynamic response of the RAT, its structures and the HIFAR core. However, some general comments can be made.

Most previous analyses assumed the most likely missile generated by an in-vessel steam explosion, would be a plug or rig ejected vertically upwards. In HIFAR these components are locked into place, therefore ejection would be unlikely. In vessel missiles are a possibility which may lead to RAT rupture. The closest boundary to the core is the plenum and RAT base which would feel the effects of an explosion generated in the core region, before the other tank boundarys. Rupture of the 2Tan tube is a possibility which would lead to a slow leak of coolant to the graphite space. If this occurred, it is likely pressure relief would be almost immediate and there would be no threat to the containment by missiles. Failure of the RAT is a possible consequence of the in core steam

explosion, as pressures indicated from observed steam explosions are of the order of magnitude where RAT failure would be likely to occur. Again, pressure relief would be very rapid.

ZAPP calculations show that to just melt fuel in HIFAR at the core centre line of the highest rated fuel element, requires a reactivity injection of 2.5$ per cent allied with a failure to SCRAM. The only possible mechanism for a reactivity accident producing enough molten fuel for a steam explosion in core would be failure of two or more CCA's practically simultaneously along with failure of the halving time trip, or failure of a single CCA and complete failure of the safety circuits at full power [Connolly and Clark, 1986]. Both these scenarios must be rated as incredible.

8. CONCLUSIONS

The modelling of two destructive reactor events due to a steam explosion has given an estimate of the efficiency of such a reaction in plate type water moderated cores, which suffer a reactivity accident under severe conditions. Questions remain about the validity of the calculations to model transient boiling heat transfer for long periods after peak power. A general conclusion is the efficient nature of steam explosions under these conditions. The likelihood of this type of event occurring in HIFAR is incredible as simultaneous failure of CCAs are needed to attain fuel melting, under the present limits.

9. ACKNOWLEDGEMENTS

The work described in this report was part of a project initiated by J.W. Connolly. The author wishes to express his appreciation for the guidance and interest given by Mr Connolly over the course of the work.

10. REFERENCES

Bankoff, S.G. [1980] - Destabilization of film boiling. *Physiochemical* Hydrodynamics **1**, 69-76.

Bird, M.J. [1984] - An experimental study of scaling in core melt/water interactions. PWR/SAWG/P(84)71.

Board, S.J., Hall, R.W., Hall, R.S. [1975] - Detonation of fuel coolant explosions. *Nature* **254**, 319-321.

Bunch, D.F. [1965] - SPERT 1 Destructive Test Series. Environmental monitoring and research studies. IDO 12039.

Clancy, B.E., Connolly, J.W., Harrington, B.V. [1975] - An analysis of power transients observed in SPERT 1 reactors. Part 1: Transients in aluminium plate-type reactors initiated at ambient temperature. AAEC/E345.

Clancy, B.E., Connolly, J.W., Harrington, B.V. [1976] - An analysis of power transients observed in SPERT 1 reactors. Part 2: Dependence of burst parameters on initial temperature and core moderation. AAEC/E383.

Clancy, B.E., Connolly, J.W. [1985] - An assessment of possible events following a loss of coolant accident in HIFAR. Unpublished ANSTO report.

Clancy, B.E. [1983] - ZAPP - A computer program for simulation of reactor power transients. AAEC/E568.

Cole, R.H. [1965] - Underwater Explosions. Dover Publications, Inc., New York.

Connolly, J.W., Clark, N. [1986] - Analysis of hypothetical loss-of-control-arm accidents in HIFAR. AAEC/E631.

El-Genk, M.S., Matthews, R.B., Bankoff, S.G. [1987] - Molten fuel-coolant interaction phenomena with application to carbide fuel safety. *Prog. Nucl. Energy*, **20**, 3, 151-198.

Fauske, H.K. [1972] - The role of nucleation in vapor explosion. *Trans. Am. Nucl. Soc.*, **15**, 813.

Fry, C.J., Robinson, C.H. [1980] - Propagating thermal interactions between molten aluminium and water. AEEW-R 1309.

Hall, C.M. [1988] - Measurement of local transient temperatures and heat fluxes in film boiling collapse. CEGB-TPRD/B/1076/R88.

HIFAR Safety Document [1972] - Restricted publication.

Jackson, J.D., Zhu, L.H., Derewnicki, K.P., Hall, W.B. [1988] - Studies of nucleation and heat transfer during fast boiling transients in water with application to molten fuel - coolant interactions. *Nucl. Energy* **27**, 21-29.

Kunze, J.F. ed. [1962] - Final report of SL-1 recovery operation, IDO 19311 and additional analysis of the SL-1 excursion. IDO 19313.

Mayhew, Y.R., Rogers, G.F.C. [1970] - Thermodynamic and transport properties of fluids. Basil Blackwell, Oxford.

Miller, R.W., Sola, A., McCardell, R.K. [1964] - Report of the SPERT 1 destructive test program on an aluminium, plate type, water-moderated reactor. IDO-16883.

Miller, R.W. [1988] - private communication.

Proctor, J.F. [1967] - Adequacy of explosion-response data in estimating reactor-vessel damage. *Nucl. Safety* **8**, 6, 565-572.

Robinson, G.S. [1987] - A guide to the AUS modular neutronics code system. AAEC/E645.

Silver, E.G. [1963] - SPERT program status report. *Nucl. Safety* 5, 2, 151-153.

SL1 Report Task Force [1962] - Nuclear incident at the SL-1 reactor. IDO-19302.

Volmer, M. [1945] - Kinetik der Phasenbildung, Edwards Brothers Inc., Ann Arbor, Mich., USA.

Warren, G.R., Rice, T.W. [1965] - An assessment of reactor safety modelling techniques based on the accident to the SL-1 boiling water reactor. AWRE R-3/65.

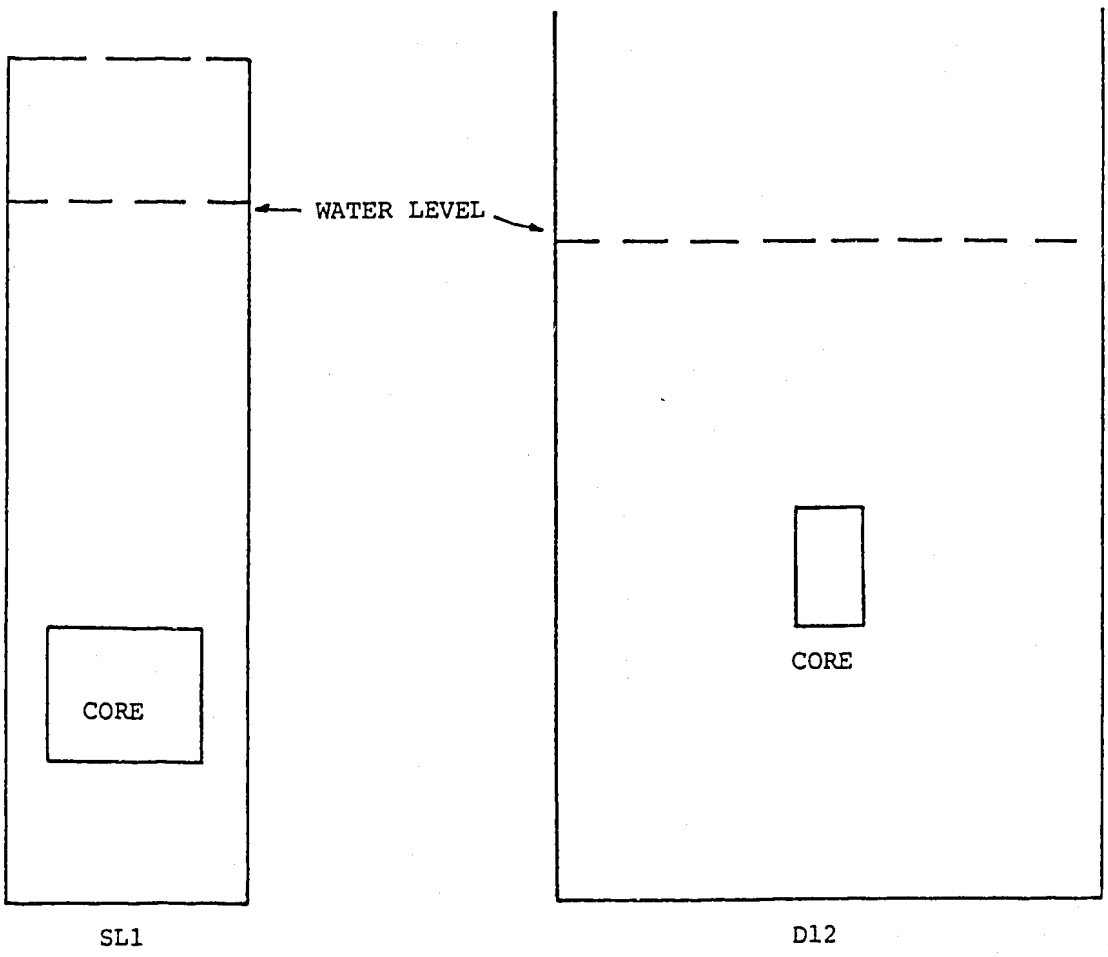

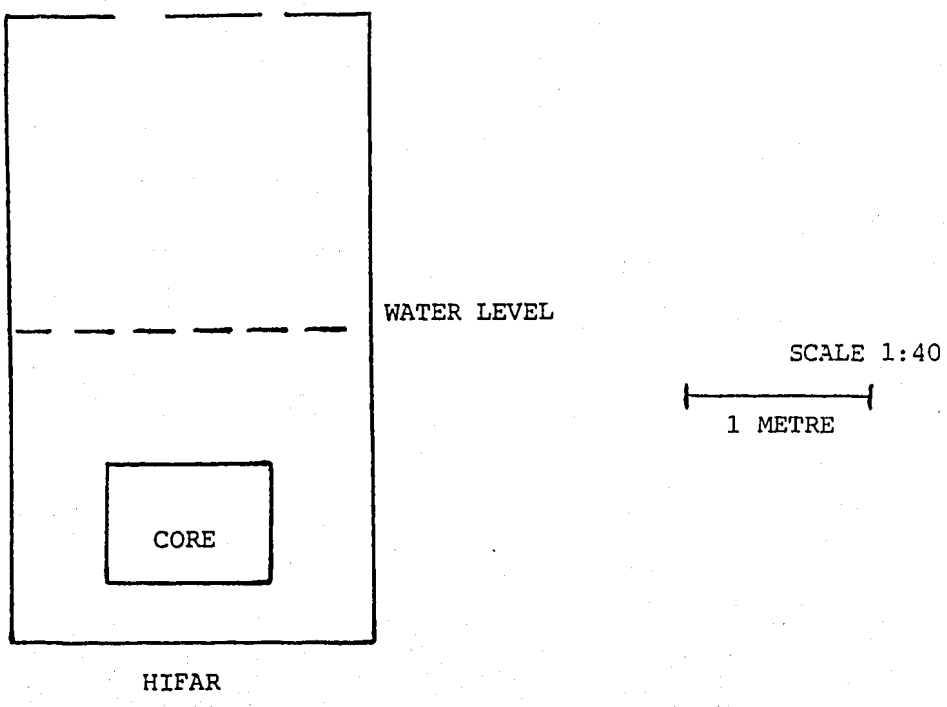

Figure 1 Scaled schematics of reactor vessels and cores

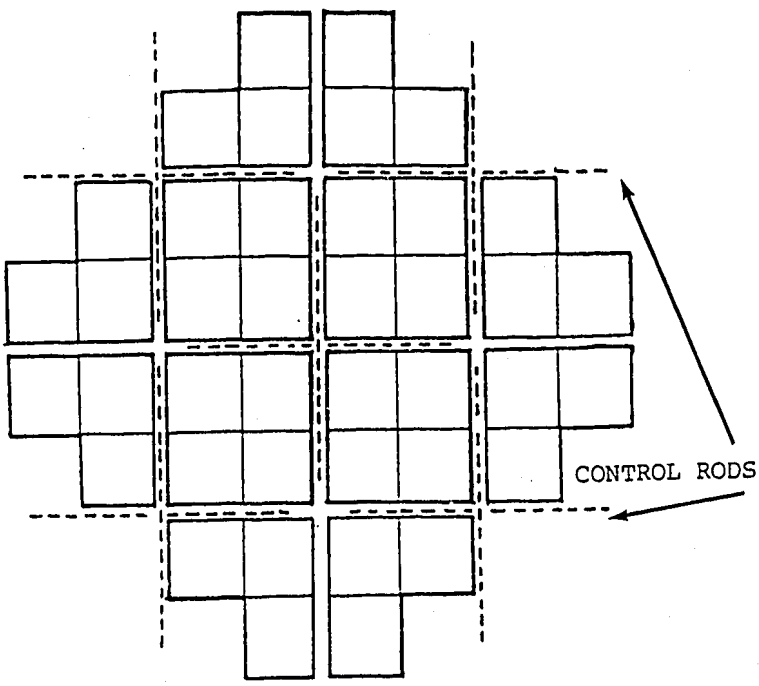

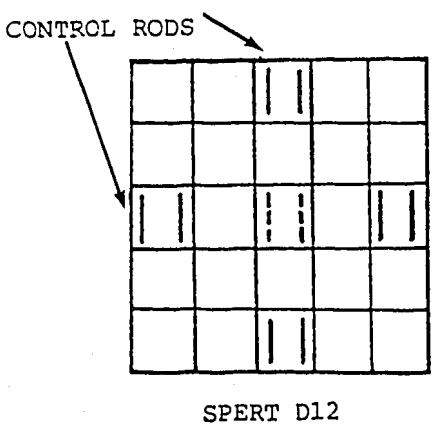

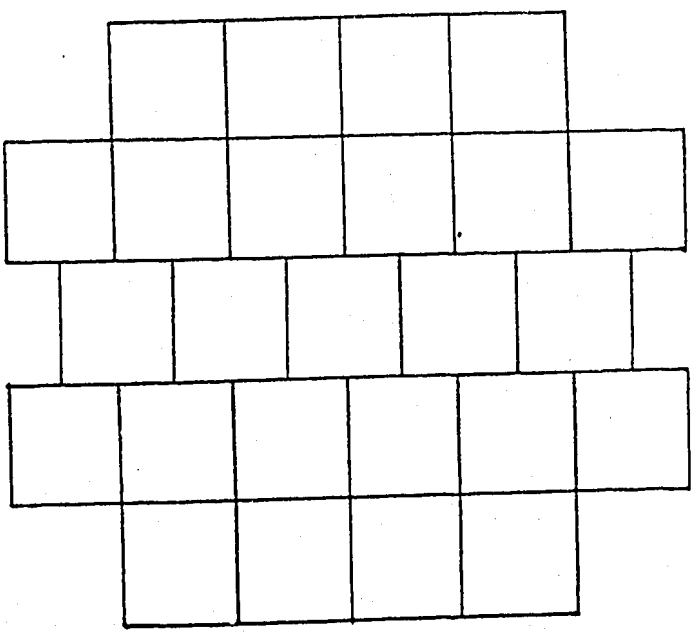

SCALE 1:10

20 cm

Figure 2 Scaled schematics of reactor core cross-section

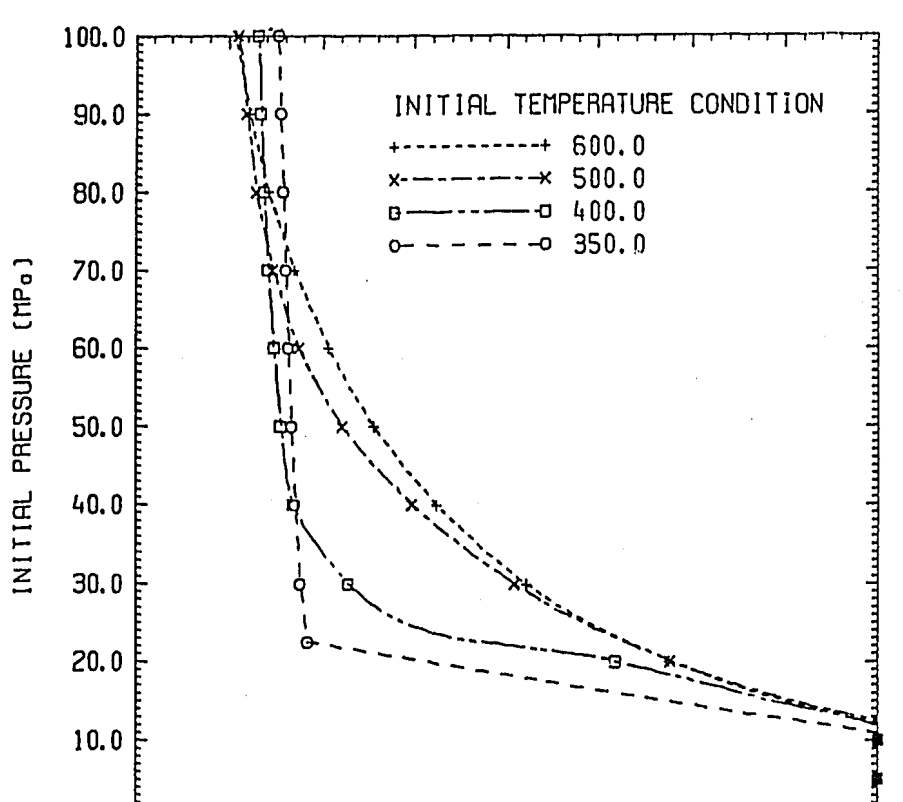

Figure 3 Initial pressure versus slug velocity

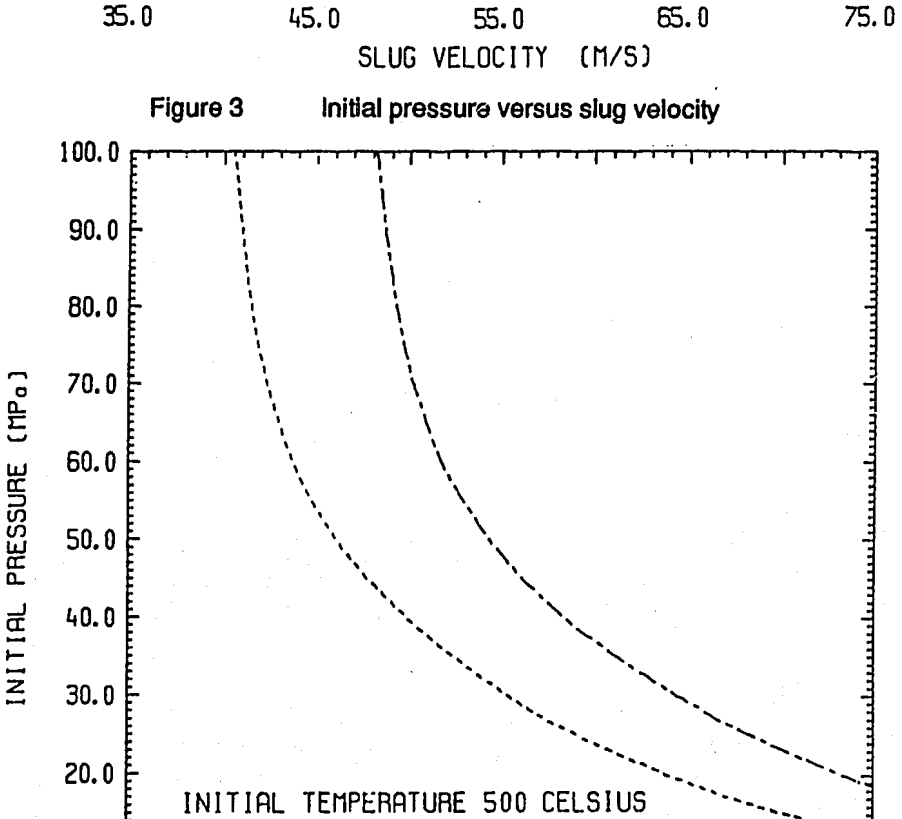

Figure 4 Initial pressure versus slug velocity (two pressure assumptions)

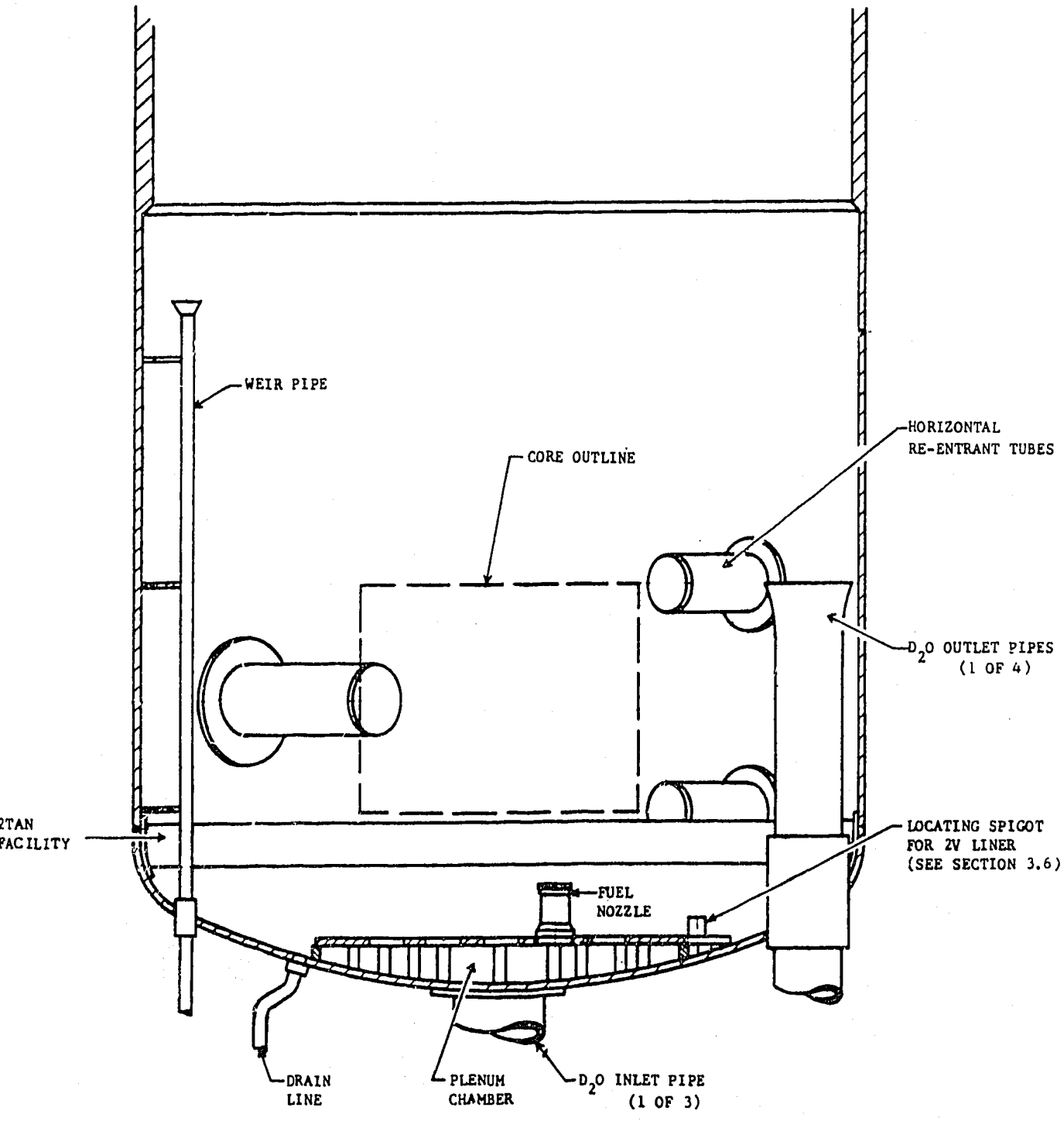

Figure 5 Reactor aluminium tank

APPENDIX A

CALCULATION OF CORE PARAMETERS AND TRANSIENT MODELLING

The modular neutronics code system AUS [Robinson 1987] was used to model the SL1 and D12 reactors, with the eventual product being core reactivity coefficients which were used after suitable modification by the reactor transient code ZAPP [Clancy 1983]. Previous work [Clancy *et al.* 1975] had established suitable reactivity coefficients for SPERT D12 reactor, and as such the following neutronic description applies to SL1.

A1. NEUTRONIC CALCULATIONS

(a) AUS Module MIRANDA

The data preparation code MIRANDA utilising the AUS.ENDFB 128 group cross-section data library was used to prepare a 50 group cross-section data set for SL1 fuel cell, fuel cladding, H_2O and an idealised 1/v neutron absorber material designated ZZ999. The calculation included a multiregion resonance treatment of the subgroup type, and a homogeneous flux solution. MIRANDA was also used to obtain 5 group cross-sections of materials in the SL1 fuel side plate.

(b) AUS Module ANAUSN

The 50 group fuel, clad and water cross-sections from (a) were used in this one-dimensional S_n transport module to obtain group fluxes for use in a group collapsing and homogenising procedure as the next calculational step.

(c) AUS Module EDITAR

The EDITAR module was used to group collapse the 50 group cross-sections from (a) to 5 groups, using as a trial solution the fluxes from (b). The 5 group cross-sections were 'smeared' to give 5 group 'fuel cell' cross-sections.

(c) AUS module POW

The two-dimensional diffusion code POW was used to develop several models of the SL1 core and its components, using the 5 group cross-sections from (a) and (c). Perturbation routines in POW were used to calculate temperature and void reactivity coefficients, and the prompt neutron lifetime of the reactors.

A2. TRANSIENT CALCULATIONS

The ZAPP code [Clancy 1983] solves the reactor kinetic equations, with a time dependent multiplication factor, k(t), and the coupling equation given by the one-dimensional heat transfer

equation

$$\frac{dn}{dt} = \left[k(t) \frac{\{1-\bar{\beta}\}-1}{\ell^*} \right] n + \sum_l \lambda_l C_l$$

$$\frac{dC_l}{dt} = \frac{k(t)\,\beta_l}{\ell^*} n - \lambda_l C_l$$

$$C \frac{\partial \theta}{\partial t} = \frac{\partial^2}{\partial x^2} K\theta + S$$

and

$$k(t) = k_o + \int_o^L dx \int_{\theta_o}^{\theta(x,t)} \frac{dk}{d\theta} d\theta$$

where n = neutron density,

$\bar{\beta}$ = effective total delayed neutron fraction,

ℓ^* = prompt neutron lifetime,

λ_l = decay constant of ith delayed neutron group,

C_l = concentration of ith delayed neutron group precursors,

β_l = delayed neutron fraction for ith delayed neutron group,

C = specific heat per unit volume,

θ = temperature,

K = thermal conductivity,

S = heat source = average fission density,

L = width of unit cell,

$\frac{dk}{d\theta}$ = temperature coefficient of reactivity per unit volume.

The reactor core was represented in 3 zones with a unit cell in each zone of 3 materials, fuel alloy, cladding and water moderator. Each unit cell could be represented by a maximum of twenty regions, two regions accounted for by fuel and cladding, with the remaining regions representing the water gap. The water gap was represented by 1 bulk water region and many fine regions adjacent to the fuel cladding. Each region in a zone is allocated a power density, temperature and void coefficient of reactivity and thermal properties of the material as part of the ZAPP input.

A model of boiling heat transfer was used to describe reactivity feedback when the moderator temperature exceeded the saturation temperature at the average zone hot spot. The conductivity of a water region is switched to a high value when its temperature exceeds a zone power weighted initiation temperature. A similar method is used to simulate voiding due to steam generation by a linear change (with temperature) to water density between 1.0 g cm^{-3} and 0.2 g cm^{-3} over a temperature range of 100°C above a void commencement temperature. The latent heat of fusion of

metal is modelled by switching the heat capacity of the metal to a high value sufficient to account for the latent heat of fusion, over a small temperature range of 10°, about the metal melting temperature.

The reactivity coefficients calculated by AUS were power weighted, and used in the ZAPP calculations, tc model the power bursts which destroyed SL1 and D12 cores.